Progress In Electromagnetics Research C, Vol. 85, 155–165, 2018

Influence of Rotor Magnet Shapes on Performance of Axial Flux Permanent Magnet Machines

Praveen Kumar* **and Rakesh K. Srivastava**

Abstract—Axial flux Permanent Magnet (AFPM) machines, due to its high torque capability, high power density and compact size, are the most suitable candidates for in-wheel Electric Vehicle application. However, the presence of cogging torque in AFPM machines, resulting from the interaction of PMs and stator slots, introduces torque ripples, noise and vibrations which deteriorates the performance of the machine. To overcome this, several techniques for cogging reduction are utilized. Out of various techniques, rotor magnet shape variation is most commonly utilized. This paper investigates the effect of some preferred magnet shaping techniques in AFPM machines on several performance parameters such as magnetic flux density distribution in air gap, cogging torque, flux linkage, no load-induced emf, emf harmonics, electromagnetic torque and torque ripple. These parameters were analyzed using 3-D Finite Element Method (FEM) based simulations. It was found that a maximum cogging reduction by 62.49% and output torque ripple by 63.25% were obtained by using short-pitched and skewed rotor magnets. This also resulted in a reduction of induced emf by 14.18% and electromagnetic torque by 15.17%.

1. INTRODUCTION

The introduction of Permanent Magnets (PM) in electrical machines has increased their torque and power capability. The advent of rare earth permanent magnets has led to further enhancement in their performance. In this category, the Axial Flux Permanent Magnet (AFPM) machines provide high level of compactness in addition to high torque, power density and torque to weight ratio. This makes it suitable for tractive and industrial applications. However, for low speed and precise positioning applications, the cogging torque phenomenon in AFPM machines becomes predominant and adversely affects their performance.

Numerous methods for cogging torque reduction in PM machines are available in literature [1–10]. These methods may be classified under two categories, namely, stator modification techniques and rotor modification techniques. The former technique includes stator slot skewing [1–3], slot opening variation [1, 4], tooth shaping [4], dummy slots/tooth [1], fractional slots per pole [1, 9] and [10], etc. The later method comprises magnet shaping [5], optimizing magnet pole arc to pole pitch ratio [1], pole arc offset [6], narrowing rotor pole embrace [7], pole-slot combination [1, 8], magnet skewing, etc. In axial flux machines, the stator laminations are spirally wound due to which cutting of slots in it is difficult. Therefore, its customized design for cogging reduction is much complex and costly [11]. Thus, the stator modification techniques are generally not employed in AFPM machines and hence, are less popular. On the other hand, most of the rotor modification techniques for cogging reduction are mainly based on magnet shape variation, which is comparatively more practical and cost-effective, and hence, more common in such machines.

Received 19 April 2018, Accepted 3 July 2018, Scheduled 16 July 2018
* Corresponding author: Praveen Kumar (praveen.rs.eee14@itbhu.ac.in).
The authors are with the Department of Electrical Engineering, IIT (BHU), Varanasi 221005, India.

The above discussed techniques necessarily reduce the cogging torque of the machine but may also affect its performance adversely. In [7], the authors have discussed the effect of narrowing pole arc embrace on cogging torque and efficiency of a PM BLDC motor. Pole arc offset technique was used in [12] to reduce harmonics and obtain sinusoidal voltage. The authors in [13] introduced slits on the stator and rotor teeth and investigated their effect on torque and efficiency of an induction motor. The efficiency of Line Start PM Synchronous motor was compared in [14] by changing the rotor pole geometry and type of magnet material. In [15] also, different PM materials were used to investigate its effect on torque and efficiency of a spherical motor. The performance comparison of internal and external rotor PM machines with same PM geometry was obtained in [16]. However, such type of study for Axial Flux PM machines has not been conducted so far.

In this paper, some common magnet shaping and displacement techniques applied to cogging reduction in AFPM machines are taken for analysis. The shapes are selected after critical literature review based on their effectiveness to achieve maximum cogging reduction. For such techniques, the performance parameters of the machine such as magnetic flux density distribution in air gap, flux linkage, no load-induced emf, emf harmonics, electromagnetic torque and torque ripple in addition to cogging torque are analysed. The objective of this analysis is to help machine designers to wisely select these modifications depending on their specific application requirement, i.e., whether the application demands smooth and noiseless operation or high output torque is required. For this analysis, a 3-D model of the machine is prepared on FEM based software and simulated. In the next section, 3-D modelling of AFPM machine has been presented. Section 3 discusses various magnet shapes selected for study. The effect of such shapes on various mentioned performance parameters of the machine has been obtained in Section 4. In Section 5, comparison of results and observation is presented. Conclusion of the paper is discussed in Section 6.

2. 3-D MODELLING OF AFPM MACHINE

To investigate the impact of various magnet shapes on the discussed performance parameters of AFPM machine, the use of software tools is a common practice. This can be cited from [17] in which computer aided design of Linear PM Synchronous machine was obtained. Software based design of electrical machines can also be referred from [2, 3, 5, 12–16]. FEM based softwares such as Ansoft Maxwell, JMAG, etc. exploit numerical method to obtain analysis results. In addition to numerical method, design modifications can also be modeled analytically as discussed in [18]. Although the analytical calculations are very accurate and provide an insight into the basic causes of cogging, AFPM machine requires mathematical deductions in 3-D which becomes much more complex. However, the FEM based software tools provide a simplified platform to model any design improvements and perform various analyses with precise results. Thus, a 3-D model of AFPM machine as shown in Figure 1 is prepared using Maxwell software to perform this study.

The model of AFPM machine shown in Figure 1 is prepared using the specifications given in Table 1. The parameters of Table 1 have been obtained using design calculations for a small-sized circular loom application motor of 750 W, 120 V, 4 A, 750 rpm. The simulation software provides option for selection of solid or laminated core for stator. In this study, laminated stator core is opted having equal angular widths of tooth and slot. 3-phase non-overlapping winding was used for stator excitation. The rotor having 8 magnet poles with a back iron is also modeled. The various analysis results are obtained using magnetostatic as well as transient analysis of the model.

The pole-slot combination of the machine is chosen in such a way to obtain maximum symmetry and minimum unbalanced magnetic pull. The machine symmetry is obtained as the Highest Common Factor (HCF) between the number of stator slots and rotor pole pairs. The higher the HCF is, the higher the machine symmetry is and the lower the unbalanced magnetic pull is.

3. MAGNET SHAPES FOR COGGING REDUCTION

As discussed earlier, the rotor modification techniques for cogging reduction are more common than stator techniques due to their reduced complexity and cost-effectiveness. The rotor techniques are mainly based on rotor magnet shape variation. From the literature review, it is observed that the short-pitching

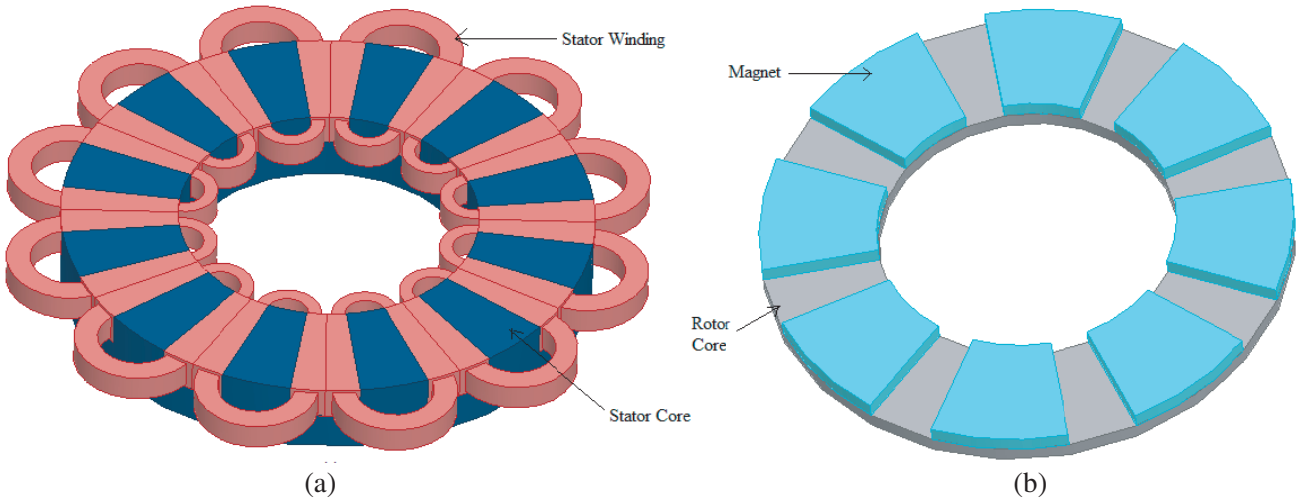

Figure 1. AFPM machine. (a) Stator. (b) Rotor.

Table 1. Specifications of AFPM machine.

Parameter	Value	Parameter	Value
Stator outer diameter, D_o	160 mm	Number of poles, $2p$	8
Stator inner diameter, D_i	90 mm	Magnet type	NdFeB
Stator core thickness, h_c	22 mm	Residual magnetism, B_r	1.2 T
Number of stator slots, Q_s	12	Thickness of magnet, h_m	5 mm
Angular slot/tooth width	15 degrees	Rotor core thickness, h_i	5 mm
Slot depth, h_s	10 mm	Supply voltage, V	120 V
Type of winding	Non-overlapping	Rated Power, P_o	750 W
Conductors per slot, N_1	150	Rated Speed, Ns	750 rpm
Number of phases, m	3	Supply frequency, f	50 Hz
Air gap length, g	1 mm	Rated current, I_o	4 A

and skewing of magnets are the most effective and commonly preferred technique for cogging reduction in both radial and axial flux machines. In addition to this, the magnet displacement technique is also utilised in axial flux machines. In view of this, such magnet shapes that contribute towards maximum cogging reduction are selected, and their influence on various performance parameters of the machine is investigated. The various magnet shapes taken are shown in Figure 2 and discussed as follows.

3.1. Short-Pitched Magnet

Figure 2(a) shows a full-pitched unskewed magnet pole. This magnet shape is taken as a reference for comparison with other magnet shapes. For an 8-pole rotor, this magnet has a pitch of 45 mechanical degrees. The pitch of this magnet can be reduced from 45 mechanical degrees by a certain ratio to obtain a short-pitched magnet as shown in Figure 2(b). It can be cited from [1] that the optimal value of pole arc to pole pitch ratio, α_p, to obtain minimum cogging torque, neglecting fringing of magnet flux, can be obtained from the expression

$$\alpha_p = \frac{N - k_1}{N}, \quad k_1 = 1, 2, \ldots, N \tag{1}$$

where $N = N_c/2p$, N_c is the least common multiple between the number of stator slots and rotor poles, p the number of rotor pole pairs, and Q_s the number of stator slots.

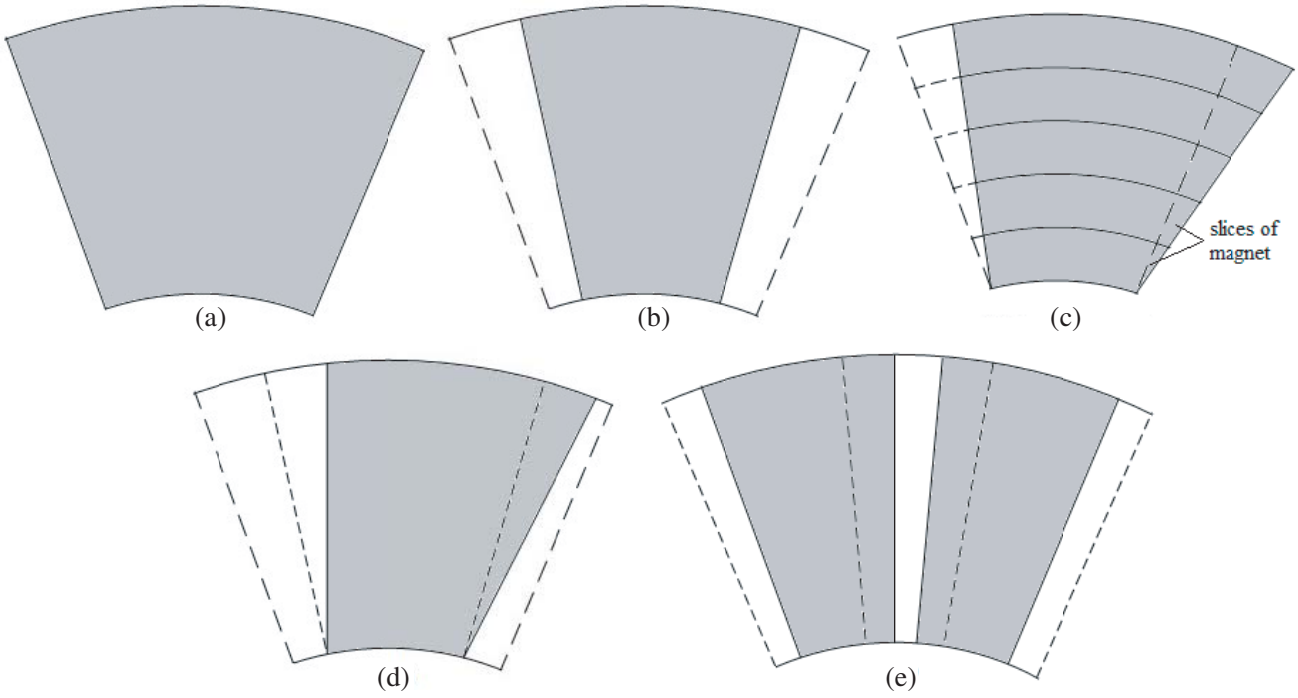

Figure 2. (a) Full-pitched unskewed magnet. (b) Short-pitched unskewed magnet. (c) Full-pitched skewed magnet. (d) Short-pitched skewed magnet. (e) Short-pitched displaced magnets.

Thus, for the specifications of AFPM machine given in Table 1, the optimal value of pole arc to pitch ratio can be calculated. For 12 slots and 8-pole combination, three possible values of α_p are obtained as 0.33, 0.67 and 1. Taking the value of α_p as high as possible to minimize the reduction in air gap flux density and output torque has also been suggested in [1]. From this point of view, the optimal value of α_p is selected as 0.67 which corresponds to 30 mechanical degrees or 120 electrical degrees.

3.2. Skewed Magnet

Magnet skewing is a technique for cogging reduction in which the slices of the regular magnet are gradually shifted as shown in Figure 2(c). The angle by which the magnet slices are shifted is referred to as skew angle. The optimal value of magnet skew angle, α_{sk}, to obtain minimum cogging torque as obtained from [1] and [5] is expressed as

$$\alpha_{sk} = \frac{kQ_s}{N_c} \times \frac{2\pi}{N_c} \quad k = 1, 2, \ldots, \frac{N_c}{Q_s} \tag{2}$$

From the above expression, the optimal value of α_{sk} for a 12 slots 8-pole machine is obtained as 7.5° and 15°. It was observed in [5] that the peak to peak value of cogging torque decreases with increase in skew angle, α_{sk}. In the present case, the maximum optimal value of α_{sk} is 15°. Hence, the skew angle of 15° has been selected for study.

3.3. Both Short-Pitched and Skewed Magnet

The combination of the above discussed magnet shaping techniques may result in a different magnet shape as shown in Figure 2(d). the resulting magnet shape can be called as both short-pitched and skewed magnet. For this technique, the optimal value of short-pitch angle, α_p, and skew angle, α_{sk}, are taken equal to those calculated in Sections 3.1 and 3.2. Thus, 120 electrical degrees short-pitched and 15 mechanical degrees skewed magnet is selected in this category.

3.4. Relative Magnet Displacement

This method is valid only for short-pitched magnets. In this method, the consecutive short-pitched magnets are displaced with respect to each other as discussed in [18]. The magnets may be shifted as shown in Figure 2(e). In this case, the short-pitching angle is taken same as that calculated earlier. The optimal displacement by one-fourth slot-pitch is selected as obtained in [18] for minimum cogging.

The cogging torque waveform obtained due to the above discussed magnet shapes is depicted in Figure 3. It can be observed that the peak value of cogging torque gets reduced from 8.37 Nm for unskewed magnet to 7.3 Nm for 15° skewed magnet. This is mainly because the cogging torque component waveforms due to each magnet get displaced slightly as a result of skewing. This causes cancelation of waveforms and hence, reduction of the resultant cogging torque. When the magnets are short-pitched, the number of tooth faced by each magnet pole at an instant gets reduced. This causes reduction in magnitude of cogging torque. For 30° mechanical short-pitched magnets, the cogging torque peak gets reduced to 3.7 Nm. For both short pitched and skewed magnets, the peak cogging torque has a minimum value of 3.14 Nm. For displaced magnets, the peak value is observed as 4.43 Nm with an increase in periodicity.

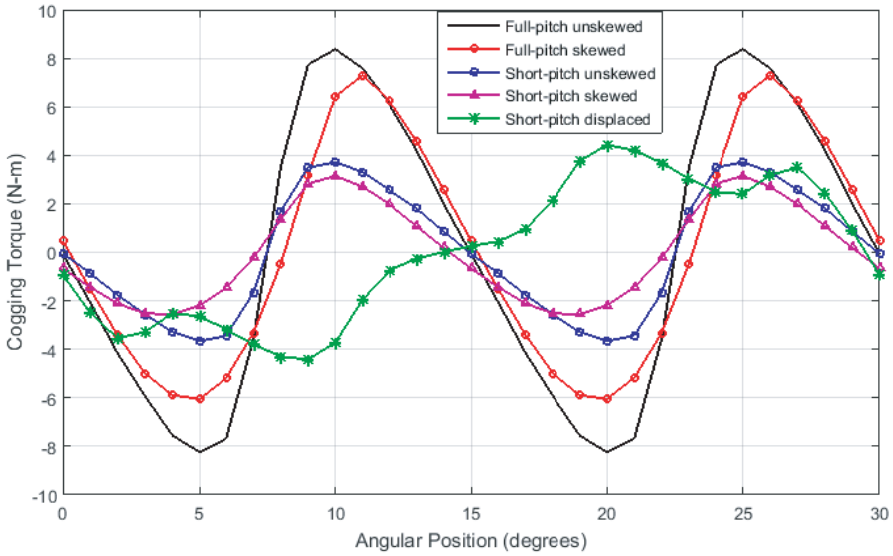

Figure 3. Cogging torque waveform due to various magnet shapes.

4. INFLUENCE OF MAGNET SHAPES ON PERFORMANCE

The magnet shapes discussed in the previous section were selected in such a way that the cogging torque reduction achieved is high. However, the machine with minimum cogging torque does not assure best performance. Thus, the magnet shapes that achieve high cogging reduction must be investigated for their effect on performance. In view of this, various performance parameters such as air gap flux density distribution, flux linkage, no load-induced emf, emf harmonics, electromagnetic torque, torque ripple and unbalanced magnetic force on stator have been analysed in this section as follows.

4.1. Air Gap Magnetic Flux Density Distribution

The variation in the shape of rotor magnet poles leads to change in the magnetic flux density distribution in the air gap. As a result, the magnitude and waveform shapes get altered. Figure 4 shows the variation in z component of air gap flux density distribution in the air gap at different radii of the machine. It can be observed from the figures that flux density waveforms at different radii overlap each other due to unskewed magnets, while the waveforms get slightly displaced due to skewed magnets. This is obvious

as the magnet slices are also shifted from their actual position. The comparison in z-component of flux density distribution in the middle of the air gap at a given radius is shown in Figure 5. It can be observed that for full-pitched magnets, the width of the peak flux density under each magnet is more than that of short-pitched magnets. Due to this, the magnitude of flux density for shot-pitched magnets gets reduced. This in turn reduces the magnitude of parameters such as induced emf and electromagnetic torque.

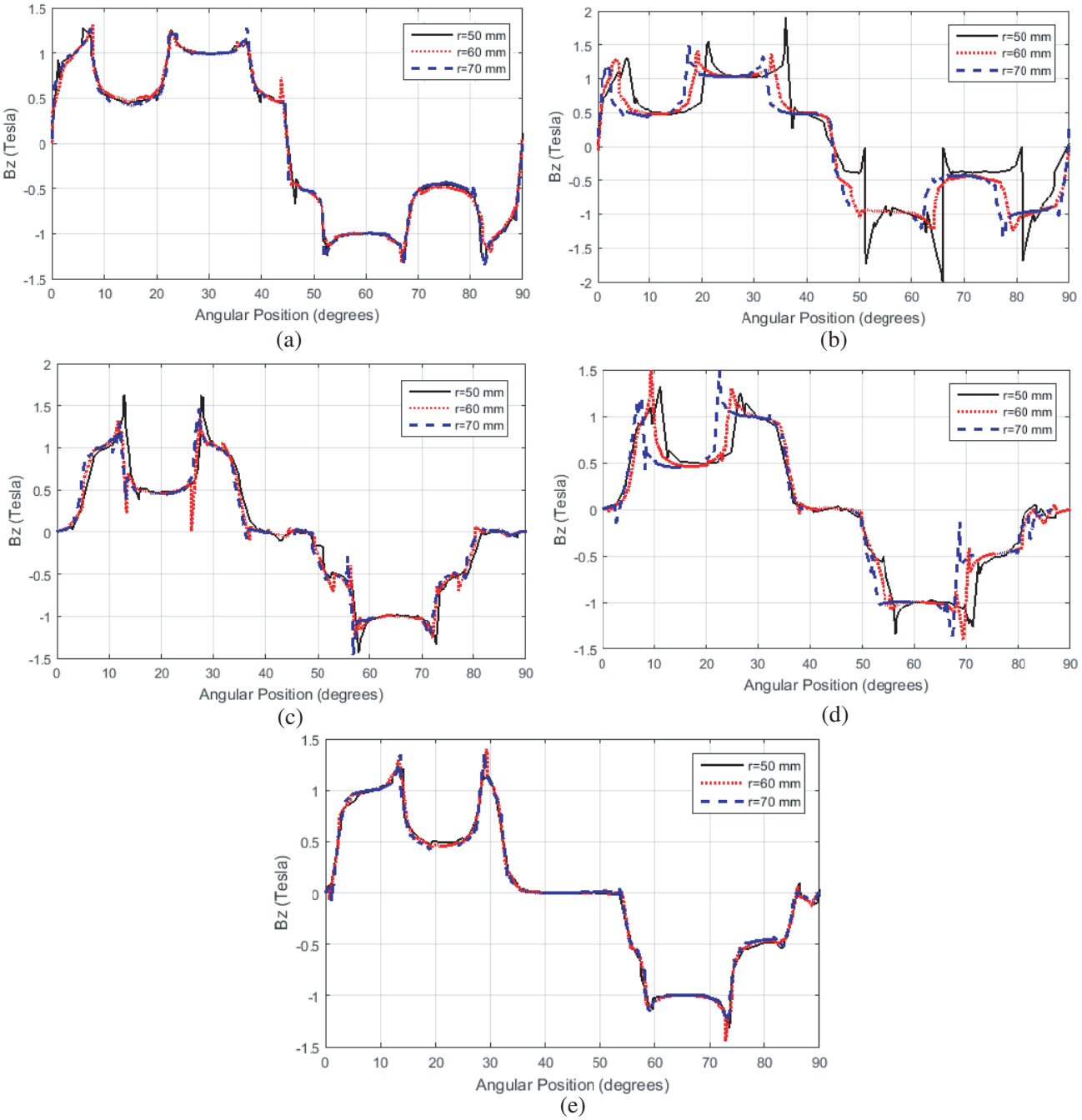

Figure 4. z-component of magnetic flux density distribution, Bz, in air gap at $z = 22.5$ mm for (a) full-pitch unskewed magnet, (b) full-pitch skewed magnet, (c) short-pitch unskewed magnet, (d) short-pitch skewed magnet, (e) short-pitch displaced magnet.

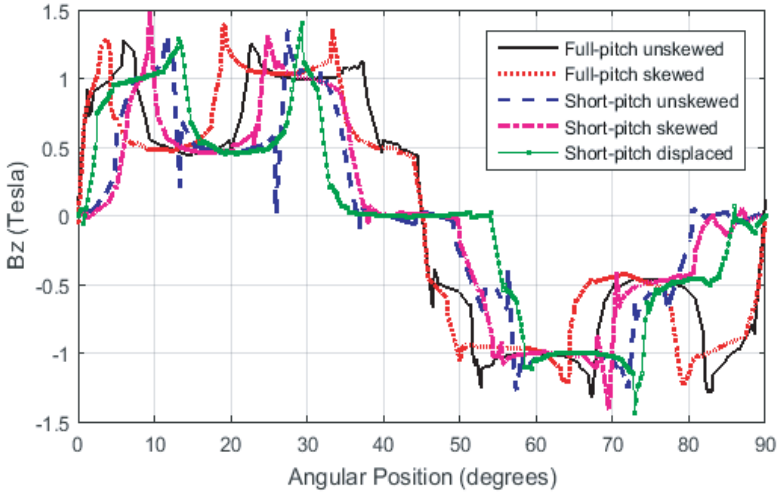

Figure 5. z-component of magnetic flux density distribution, Bz, in air gap at $z = 22.5\,\text{mm}$ and $r = 60\,\text{mm}$ for various cogging reduction techniques.

4.2. Flux Linkage

The magnet shape variation also affects the flux linkage through the stator windings of the machine. When the magnets are short-pitched, the gap between two consecutive magnet poles increases. This causes increase in magnet leakage flux. Thus, the magnitude of linkage flux through the stator windings decreases. This is illustrated in Figure 6 which shows the variation of flux linkage with rotor mechanical position. It can be observed from the figure that the peak of flux linkage waveform for full-pitched magnets is higher than that for short-pitched magnets. For displaced magnets, the flux linkage waveform is also slightly displaced with respect to other waveforms.

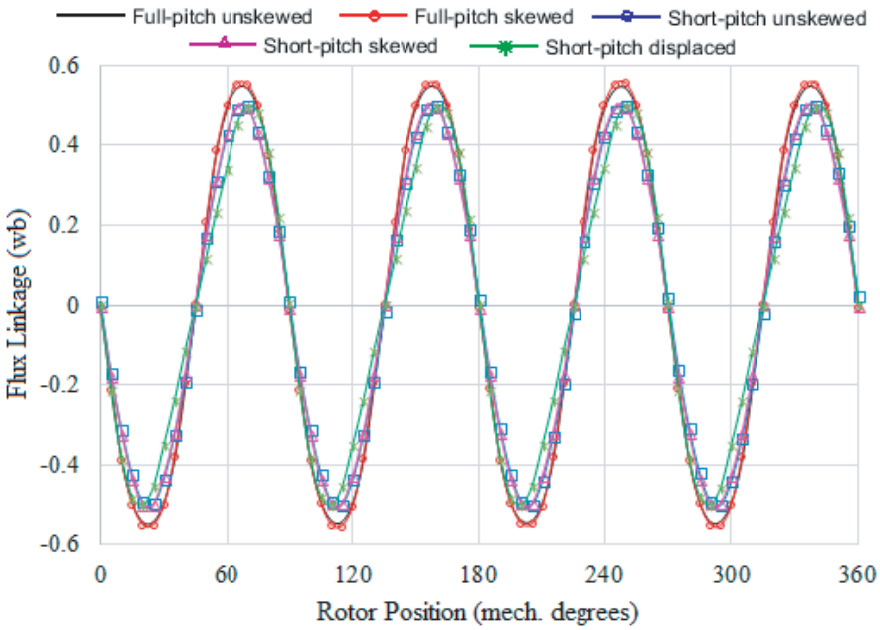

Figure 6. Flux linkage versus rotor position for various rotor magnet shapes.

4.3. No Load Induced emf

The no load induced emf in the stator windings of a machine is totally dependent on the air gap flux density distribution, flux linkage and rotor speed. As discussed earlier in Sections 4.1 and 4.2, the variation in rotor magnet shapes from full-pitch to short pitch reduces the amplitude of air gap flux density and flux linkage, while magnet skewing distorts their waveform shape. The no load induced emf in the windings also follows the same pattern. It can be elucidated from Figure 7 that the peak value of no load induced emf at 750 rpm for full pitched magnets is the highest, having a value of 190 V for full-

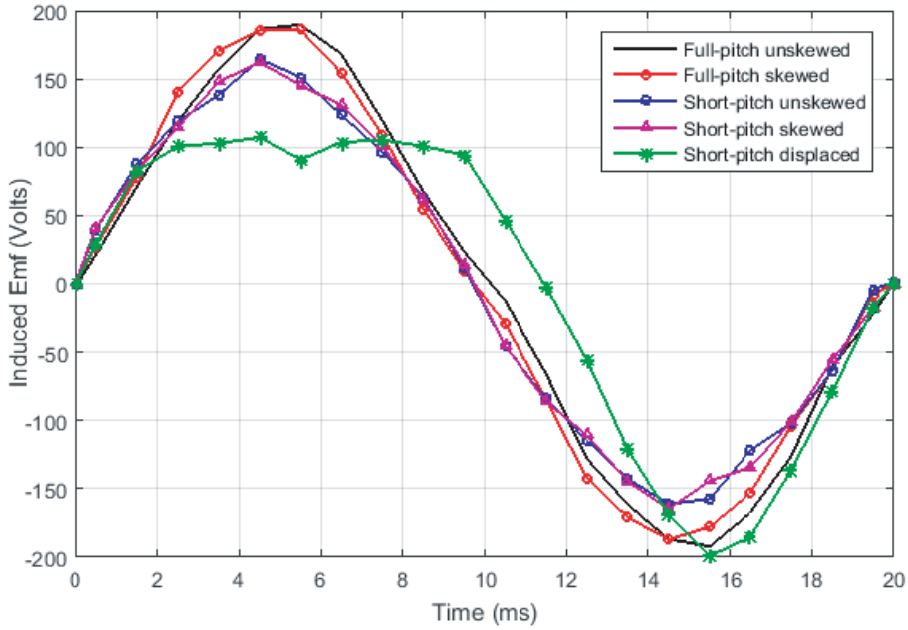

Figure 7. Per phase no-load induced emf waveform at 750 rpm.

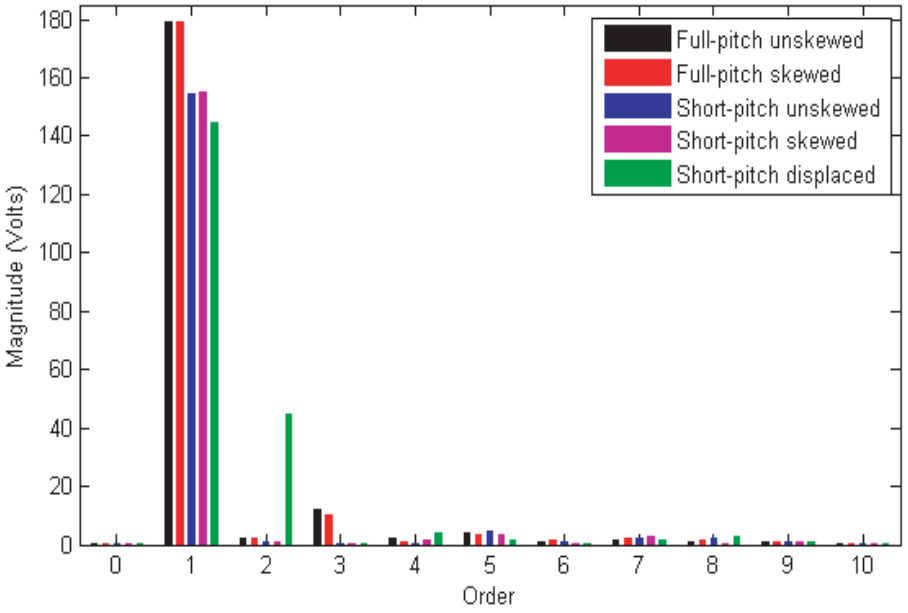

Figure 8. FFT of per phase no load induced emf waveforms.

pitched unskewed magnets and 186 V for full-pitched skewed magnets. As the magnets are short-pitched, the emf amplitude is reduced to 164 V for short-pitched unskewed magnets and 162 V for short-pitched skewed magnets. For displaced magnets, the waveform shape becomes highly unsymmetrical having a positive peak of 107 V and negative peak of 200 V. This is mainly due to high leakage flux at the position where the gap between the magnets becomes large due to displacement.

The Fast Fourier Transform (FFT) of the voltage waveforms is shown in Figure 8. It can be seen from the figure that the fundamental harmonics of induced emf also presents a similar pattern as already discussed. For displaced magnets, the second harmonics component is high due to the unsymmetrical magnet placement and is also reflected in the emf waveform.

4.4. Electromagnetic Torque and Torque Ripple

The electromagnetic torque of the machine at rated load current of 4 A for different magnet shapes is obtained as shown in Figure 9. Since the discussed variations in magnet shapes causes reduction in net magnitude of air gap flux density and also distorts its waveform shape, the electromagnetic torque, being proportional to air gap flux density, also gets deteriorated accordingly. It was found that the average electromagnetic torque for full-pitched unskewed magnet rotor was 19.24 Nm, and that for full-pitched skewed magnets was 18.31 Nm. When short-pitched magnets are used, the torque becomes 16.96 Nm for short-pitched unskewed magnet and 16.32 Nm for short-pitch skewed magnets, which is minimum among the discussed magnet shapes. For displaced magnets, torque is obtained as 16.78 Nm. Thus, it can be inferred that although the discussed magnet shapes attain significant cogging reduction, a compromise in electromagnetic torque must be tolerated.

Figure 9. Electromagnetic torque versus rotor position for different rotor magnet shapes.

Since the discussed magnet shapes achieve considerable cogging torque reduction, the improvement in electromagnetic torque ripple is evident. It can be observed form Table 2 that the peak to peak value of electormagnetic torque gets reduced from 19.29 Nm for full-pitch unskewed magnet to 7.09 Nm for short-pitched and skewed magnet, which corresponds to a reduction by 63.25%.

5. COMPARISON AND OBSERVATION

The comparison of various performance parameters of AFPM machine due to variation in magnet shapes is presented in Table 2. The presented comparison is based on the percentage reduction obtained in

Table 2. Comparison of performance parameters of AFPM machine for various magnet shaping techniques.

Magnet shaping techniques		Cogging Torque		Per phase induced emf		Electromagnetic Torque		Electromagnetic Torque ripple	
α_p	α_{sk} (mech. degrees)	Peak value (N-m)	% Reduction	Rms value (Volts)	% Reduction	Average Value (Nm)	% Reduction	Peak to peak Value (Nm)	% Reduction
1	0°	8.37	-	128.44	-	19.24	-	19.29	-
1	15°	7.3	12.78	127.7	0.57	18.31	4.83	16.42	14.88
0.67	0°	3.7	55.79	110.54	13.94	16.96	11.85	11.64	39.66
0.67	15°	3.14	62.49	110.23	14.18	16.32	15.17	7.09	63.25
0.67	0°	4.43	47.07	108.68	15.38	16.78	12.78	13.29	31.1
3.75° displaced									

each parameter because of variation in rotor magnet shapes. It can be observed from the table that the AFPM machine with 120° short-pitched and 15° skewed rotor magnets has a maximum cogging reduction by 62.49% as compared to the machine having full-pitched unskewed magnets. However, the per phase no load induced emf and electromagnetic torque for this machine also shows a degradation by 14.18% and 15.17%, respectively. The output torque ripple got reduced by 63.25% which is a much significant achievement to attain smooth and noiseless operation. Other magnet shapes also show a similar variation in performance parameters. For displaced magnets, in addition to torque ripple reduction and performance deterioration, harmonics are also introduced in the emf waveform. This is not recommended from the point of view of reduction in power factor.

6. CONCLUSION

In this paper, several magnet shapes commonly utilised for cogging torque reduction in AFPM machine were discussed and their effect on the performance of the machine was investigated. For this, Finite Element Analysis of the machine was performed in 3-D using Maxwell software, and the performance parameters such as flux density distribution, flux linkage, no load induced emf, electromagnetic torque and torque ripple were evaluated. It was found that among various discussed magnet shapes, a maximum reduction of 62.49% in cogging torque and 63.25% in output torque ripple was observed by simultaneous short-pitching and skewing of rotor magnets. However, the air gap magnetic flux density and winding flux linkages also got reduced which resulted in decrement of induced emf and output torque by 14.18% and 15.17%. From this analysis, it can be concluded that although the discussed magnet shapes may be best suited for minimizing cogging torque and torque ripples, they may not furnish best performance. There always exists a trade-off between output torque and torque ripple. Thus, a compromise must be made between output torque and torque ripples of the machine depending on specific application requirements.

REFERENCES

1. Zhu, Z. Q. and D. Howe, "Influence of design parameters on cogging torque in permanent magnet motors," *IEEE Trans. Energy Convers.*, Vol. 15, No. 4, 407–412, Dec. 2000.
2. Bianchi, N. and S. Bolognani, "Design techniques for reducing the cogging torque in surface-mounted PM motors," *IEEE Trans. Ind. Appl.*, Vol. 38, No. 2, 1259–1265, Sep./Oct. 2002.
3. Aydin, M., "Magnet skew in cogging torque minimization of axial gap permanent magnet motors," *Proc. IEEE ICEM*, 1–6, Vilamoura, Portugal, Sep. 2008.

4. Wanjiku, J., M. A. Khan, P. S. Barendse, and P. Pillay, "Influence of slot openings and tooth profile on cogging torque in axial-flux PM machines," *IEEE Trans. Ind. Electron.*, Vol. 62, No. 12, 7578–7589, Dec. 2015.
5. Aydin, M., Z. Q. Zhu, T. A. Lipo, and D. Howe, "Minimization of cogging torque in axial flux permanent magnet machines — Design concepts," *IEEE Trans. Magn.*, Vol. 43, No. 9, 3614–3622, Sep. 2007.
6. Ocak, C., İ. Tarımer, and A. Dalcalı, "Advancing pole arc offset points in designing an optimal PM generator," *TEM Journal*, Vol. 5, No. 2, 126–132, 2016.
7. Ocak, C., İ. Tarımer, A. Dalcalı, and D. Uygun, "Investigation effects of narrowing rotor pole embrace to efficiency and cogging torque at PM BLDC motor," *TEM Journal*, Vol. 5, No. 1, 25–31, 2016.
8. Libert, F. and J. Soulard, "Investigation on pole-slot combinations for permanent-magnet machines with concentrated windings," *Proc. IEEE ICEM*, 5–8, Cracow, Poland, Sep. 2004.
9. Güemes, J. A., A. M. Iraolagoitia, P. Fernández, and M. P. Donsión, "Comparative study of PMSM with integer-slot and fractional-slot windings," *2010 XIX International Conference on Electrical Machines (ICEM)*, 1–6, 2010.
10. Li, J., D.-W. Choi, S.-G. Lee, J.-H. Jang, and Y.-H. Cho, "Minimization of cogging torque in fractional-slot axial flux permanent magnet synchronous machine with conventional structure," *Proc. IEEE ICEF*, 1–4, Dalian, China, 2012.
11. Aydin, M. and M. Gulec, "Reduction of cogging torque in double-rotor axial-flux permanent-magnet disk motors: A review of cost-effective magnet-skewing techniques with experimental verification," *IEEE Trans. Ind. Electron.*, Vol. 61, No. 9, 5025–5034, Sep. 2014.
12. Tarımer, I., S. Sakar, and A. Dalcalı, "Effects of structural design of pole arc offset in a salient pole generator to obtaining sinusoidal voltages with the least harmonics," *Przegląd Elektrotechniczny*, R. 86, 367–372, NR 11a/2010, 2010.
13. Arslan, S., S. A. Oy, and İ. Tarımer, "Investigation of stator and rotor slits' effects to the torque and efficiency of an induction motor," *TEM Journal*, No. 1, 117–125, Feb. 2017.
14. Tarımer, İ., "Investigation of the effects of rotor pole geometry and permanent magnet to line start permanent magnet synchronous motor's efficiency," *Elektronika Ir Elektrotechnika*, Vol. 90, No. 2, 67–72, 2009.
15. Tarımer, İ. and A. Dalcalı, "Effects of permanent magnets on torque and power density of spherical motors," *TTEM (Technics Technologies Education Management)*, Vol. 10, No. 2, 144–149, 2015.
16. Tarımer, İ. and C. Ocak, "Performance comparison of internal and external rotor structured wind generators mounted from same permanent magnets on same geometry," *Elektronika Ir Elektrotechnika*, Vol. 92, No. 4, 65–70, 2009.
17. Tarımer, İ., S. Sakar, and A. Dalcalı, "Computer aided design of permanent magnet linear synchronous generator," *Przegląd Elektrotechniczny*, R. 86, 230–234, NR 3/2010, 2010.
18. Tiegna, H., Y. Amara, and G. Barakat, "Study of cogging torque in axial flux permanent magnet machines using an analytical model," *IEEE Trans. Magn.*, Vol. 50, No. 2, Art. ID. 7020904, Feb. 2014.